

Turbulent Boundary Layer Manipulation using Synthetic Jet Actuation

Adnan Qayoum, Vaibhav Gupta, and P.K.Panigrahi

Abstract— Synthetic jet actuator shows great promise as active flow control device. The aim of this study is to understand the interaction of vortical structures produced by a round synthetic jet with the turbulent boundary layer. The synthetic jet is obtained by piezo-electric actuation in both sinusoidal and amplitude modulation mode. The quantitative picture about the nature of interaction has been obtained from the liquid crystal images for different actuation parameters. Detailed hotwire measurements have been carried out to understand the mean flow and fluctuation field development due to the interaction between the vortical structures of the synthetic jet and that of the turbulent boundary layer. Overall increase in heat transfer coefficient and decrease in turbulent shear stress is observed due to the synthetic jet actuation.

Keywords— Synthetic jet actuator, piezoelectric, Liquid Crystal Thermography (LCT), boundary layer

I. INTRODUCTION

A lot of attention has been paid in the literature to crossflow jets because they are used in many practical applications like film cooling in turbine, fuel injection, pollutant emission, etc. The objectives of each application are different, for film cooling, the goal is to keep the jet attached to the wall, whereas for fuel injection the aim is to enhance the mixing. A jet issuing into a crossflow exhibits a rich and complex structure as the fluid from the two streams meet and interact. Arguably the most interesting feature of a jet issuing into a crossflow is the counter rotating vortex pair that is formed from the crossflow interaction. If the jet trajectory and the vortex pair remain confined into the boundary-layer region of the flow, then the jet/boundary-layer interaction has an effect similar to a passive vortex generator. The vortex pair transports high-momentum fluid at the edge of the boundary layer to the near-wall region, creating a fuller velocity profile that is better resistant to separation. The formation mechanism of the counter-rotating vortex pair downstream of the jet has been studied extensively and has given rise to many debates (Kelso *et al.* [1]; Haven & Kurosaka [2]; Cortelezzi & Karagozian [3]. All of these studies have focused on steady jet. Periodic excitation of the jet has also received some interest initially for the study of vortex rings formation (Glezer [4]) or for

the penetration and the mixing enhancement of jets in crossflows (M'Closkey [5]). Synthetic jets are actuators that have been proven to effectively control separation, enhance mixing and vector thrust. The advantage of synthetic jets with respect to steady blowing or suction is that they need less momentum by one or two orders of magnitude to achieve equivalent effects. They also do not require a complex plumbing system because the momentum expulsion is only caused by the periodic motion of a diaphragm.

Smith [6] carried an experimental investigation of the interaction between a synthetic jet actuator array and a turbulent boundary layer for studying the effect of the orientation of the jet orifice. Two orientation of the actuator array with respect to the cross flow direction were studied. It was found that in the spanwise configuration the boundary layer was characterized by a wake-like region due to blockage effect while in the streamwise configuration the flow structure was consistent with the presence of longitudinal vortices embedded in the boundary layer. Rathnasingham *et al.* [7] performed a real time synthetic jet based active control of flat plate turbulent boundary layer using system identification approach. The coherent structures were identified from the wall based sensors that measured wall shear, using conditioned spectral analysis. Combining the prediction and the effect of the actuator, the control input to the actuator was generated. With this scheme, they reported a reduction in wall pressure fluctuations by 15%, wall shear stress by 7% and bursting frequency (obtained by application of VITA method to wall pressure and velocity signals) up to 23%. Milanovic & Zamman [8] carried experimental investigation on synthetic jets, with and without crossflow from orifices of different geometry. They found that for synthetic jet in crossflow, the distributions of mean velocity, streamwise vorticity, as well as turbulence intensity are similar to those of a steady jet in crossflow. It is clear from the literature review that although the synthetic jets have found wide applications in active control of separation, mixing enhancement in jets etc., there is minimal understanding about the mechanisms by which synthetic jet actuation modifies the structure of a boundary layer in turbulent flows.

II. EXPERIMENTAL DETAILS AND DATA REDUCTION

The experimental setup primarily consists of a flow circuit, liquid crystal/imaging system, synthetic jet actuator and hot wire anemometry.

A. Flow Circuit

Fig. 1 shows the full schematic of the experimental setup

Adnan Qayoum is with the Mechanical Engineering Department, Indian Institute of Technology, Kanpur, India, on leave from National Institute of Technology Srinagar, Srinagar, Kashmir India (phone: +919419016328; e-mail: adnan@iitk.ac.in).

Vaibhav Gupta, was with Mechanical Engineering Department, Indian Institute of Technology Kanpur, Kanpur, India. He is now with Tata Motors, Pune, India.

P. K. Panigrahi is with the Mechanical Engineering Department, Indian Institute of Technology, Kanpur, India (e-mail: panig@iitk.ac.in).

which consists of a serpentine test passage. Air is sucked into the test section through a honey comb section, anti turbulence screen and a nozzle with 3:1 contraction ratio. The test section is 8 cm square cross-section and 100 cm long. The test section is made of Plexiglas, with top width surface made of glass for better visualization. The test section is surrounded by a plexiglas enclosure of dimensions 43cm x 40cm x 145cm. Three filament heaters placed inside the enclosure are connected to variable power supply for heating the test cell. Three fans are also mounted inside the enclosure for uniform mixing of hot air inside the enclosure. A 5 HP blower is used for generating the flow whose speed is varied with the help of a speed controller (Victor G1000) supplied by Kirolskar Electric. The blower is connected to the cell via a three way valve. The three way valve is used to initiate transient cooling inside the cell by sudden introduction of flow inside the test section. The experiments have been carried out at Reynolds number of 5500 corresponding to the average velocity of 1.1 m/s. The free stream turbulence at this working Reynolds number is equal to 0.32 percent.

B. Liquid crystal thermography

Liquid crystal (Hall Crest Inc.) designated as R30C5WA with 5oC band in the temperature range of 30-35oC has been used. The test section is illuminated by two 50W tungsten-halogen lamps. A 3-CCD color camera (SONY XC-003P) of 768 (horizontal) x 574 (vertical) pixels resolution with 16mm focal length lens (VCL-16WM) is mounted above the test section on a rail. A 24-bit true color frame grabber (Imaging Technology Inc. IC-PCI) with a personal computer is used for acquisition of the liquid crystal images.

The liquid crystal images have been for heat transfer coefficient calculation. For heat transfer coefficient calculation, the transient temperature distribution is used for the time duration till the validity of the semi-infinite solid assumption. For calibration of the liquid crystals the test surface is heated to different temperature by adjusting the input voltage to the heater. The color image of the thermocouple test surface and the reading is captured at different temperatures. The thermocouples are connected to DAQ card (National Instruments, NI) for recording. The hue (H) corresponding to the RGB values of the RGB values of the color image is calculated using the following formula.

$$H = \cos^{-1} \left\{ \frac{\frac{1}{2}[(R-G) + (R-B)]}{[(R-G)^2 + (R-B)(G-B)]^{1/2}} \right\} \quad (1)$$

where R, G and B represent red, green and blue values respectively

The relationship between hue and temperature are used for extraction of temperature from the color images. The transient cooling technique for determination of surface heat transfer coefficient uses a 1-D semi-infinite solid heat transfer model of the test surface. The criterion for validity of the semi-infinite solid assumption is that the minimum thickness of the material should be greater than $4\sqrt{\alpha t}$, where α the thermal diffusivity of plexiglas and t is the

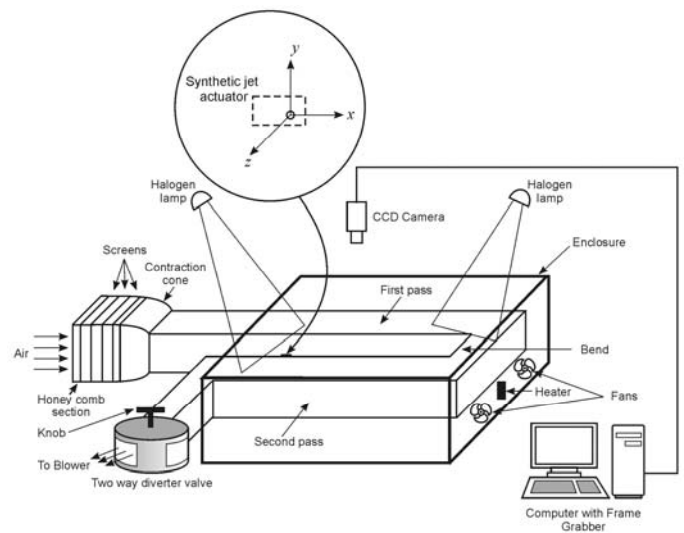


Fig. 1 The schematic of the experimental setup and the coordinate system of the synthetic jet

total duration of transient experiment. The maximum duration of a typical transient experiment in our case is 120 s. A simple calculation with the standard physical properties of plexiglas reveals that the maximum permissible penetration time of the 20 mm thick plexiglas is of the order of 225 s, which is much larger than the duration of our experiment.

Two thermocouples are used for measuring the time-dependent variations of the main-stream temperature at the inlet and the outlet of the test-section. The axial variation of mainstream temperature in the channel is interpolated from these two temperatures. The influence of gradual changes in the mainstream temperature is modeled using Duhamel's superposition theorem as:

$$T_i - T_w = \sum_{j=1}^N \left[1 - \exp\left(-\frac{h^2 \alpha (t - \tau_j)}{k^2}\right) \operatorname{erfc}\left(\frac{h \sqrt{\alpha (t - \tau_j)}}{k}\right) \right] [\Delta T_{m(j-1,j)}] \quad (2)$$

where $\Delta T_{m(j-1,j)}$ and τ_j are the temperature and time step changes respectively, T_i is the initial temperature of the test surface, T_w is the surface temperature at time t and T_m is the mainstream temperature.

During the experiment the test-section is pre-heated to a constant temperature using heaters and fans for mixing. The blower is operated at the required speed and the ambient airflow is suddenly introduced into the channel by operating the diverter valve. The transient LCT images of the test-section are recorded in the form of sequential images. The calibration equation is used to obtain the transient temperature distribution and heat transfer coefficient distribution using the above expression.

C. Synthetic jet actuator

The synthetic jet actuator is flush mounted at the bottom wall of the channel. The synthetic jet is actuated by a

resonant cantilever type oscillating member, which is set into forced oscillations by a piezo element that deforms on the application of the electric field. The deformation of the element can be controlled by adjusting the excitation voltage amplitude. The dimension of the cantilever aluminum plate is 70 mm x 26 mm x 0.35 mm. A hole is located on the top of the cavity above the cantilever tip i.e. at the location of maximum displacement of the cantilever. The orifice diameter, orifice length and cavity height are equal to 2 mm. The resonant frequency of the cantilever is equal to 475 Hz. The piezo-actuator drive unit (Spranktronics, Bangalore) amplifies the excitation signal from the function generator (Hewlett Packard, HP33120A) to the desired level and supplies to the piezo-electric element. The function generator sends both sinusoidal and amplitude modulated wave form to the piezo actuator drive unit.

Two independent dimensionless parameters are used for characterization of synthetic jet in quiescent condition. One parameter is the jet Reynolds number $Re_j (=U_o D/\nu)$ and the other is dimensionless stroke length $L (=L_o/D=U_o/fD)$

where, U_o is the time-averaged blowing velocity over the entire cycle, L_o is jet stroke length in quiescent air.

Strouhal number $(=fD/U_o)$ is another representation of reciprocal of the non-dimensional stroke length indicating the length of the fluid column expelled during the blowing stroke from the orifice Table 1 shows the values dimensionless parameters used of the synthetic jet used.

D. Hot wire anemometry

Hot wire anemometry (DANTEC 56C17) has been used for measurement of velocity and its fluctuations. DANTEC Type-55P63 X-wire probe mounted on a computer controlled traversing mechanism has been used for 2-D instantaneous velocity measurements. Both the wires were operated in constant temperature mode at 180° C. The data acquisition has been carried out using a Keithley data acquisition board KPCI 3108 in a Labview Platform. Data processing to calculate various quantities like signal mean, rms, power spectra, signal filtering etc. was carried out using separately configured VIs.

TABLE 1

Values of dimensionless parameters at different excitation voltages

V_{exc} (volts)	U_o (m/s)	Re_j	VR	L	St
20	0.21	27	0.16	0.22	4.54
30	0.45	56	0.33	0.47	2.14
55	0.93	120	0.68	0.98	1.01

III. RESULTS AND DISCUSSION

The results of synthetic jet applied to a turbulent boundary layer developing on the bottom wall of a test section at the entrance are presented. The aim of this study was to investigate the type of vortical structures that are produced by a round synthetic jet, and their interaction with a turbulent cross flow. The information about the interaction between synthetic jet and the turbulent cross flow is

important for proposing optimum flow control strategies. Therefore, the non-dimensional parameters of the synthetic jet and velocity distribution (mean & rms) inside the jet are required. The surface heat transfer coefficient distribution for different synthetic jet parameters can provide the effectiveness of synthetic jet for heat transfer enhancement technique. The influence of synthetic jet on mean and fluctuating velocity field in a turbulent boundary layer can provide information on overall interaction between the vortex structure of the synthetic jet and turbulent boundary layer.

A. Base flow measurements

Two 3 mm trips have been mounted on the bottom and top walls at the entry region of the test section for making the flow turbulent. To verify the nature of boundary layer developed after tripping, the experimental velocity profile for the base flow case in wall coordinates has been compared with that of Blasius profile and law of the wall. The profile has been measured at the immediate upstream location of the synthetic jet orifice. Fig. 2 shows the profile to be very close to the Law of the wall, which ensures the turbulent nature of the wall boundary layer. The good comparison between the two indicates the turbulent nature of the developing boundary layer on the test surface.

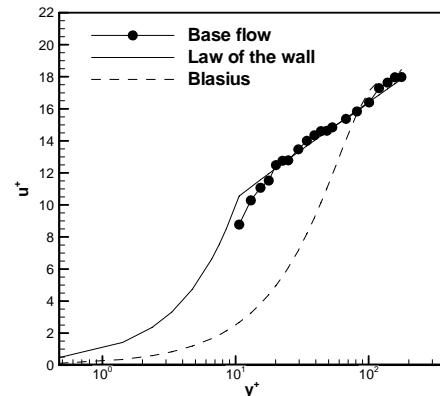


Fig. 2 Comparison of experimental wall boundary layer profile with that of turbulent law of the wall profiles

B. Synthetic jet characterization

To evaluate the characteristics of the synthetic jet hot wire measurements were carried for different actuation parameters. The velocity-time series data measured by hot wire are presented in Fig. 3 for the same actuation cases. For the amplitude modulated cases in all the figures the difference between the maximum and minimum velocities varies significantly around the mean value. As the axial distance from the orifice increases, the jet attenuates in magnitude but sustain their time period of execution cycle. The interval between two cycles for each amplitude modulated case is the reciprocal of the amplitude modulated frequency.

C. Heat Transfer measurements

Fig. 4(a) shows contour plot of heat transfer coefficient in streamwise direction. The contour plot shows high heat transfer streaks. Fig. 4(b) shows the variation of average heat transfer coefficient in streamwise direction for different

operating conditions of the synthetic jet. On account of interaction of synthetic jet with the turbulent boundary layer the heat transfer coefficient shows a significant increase. Near the orifice of the synthetic jet as expected the increase is more as compared to the downstream regions. For synthetic jet operating at a voltage of 55 volts shows high values of heat transfer coefficient at all streamwise locations.

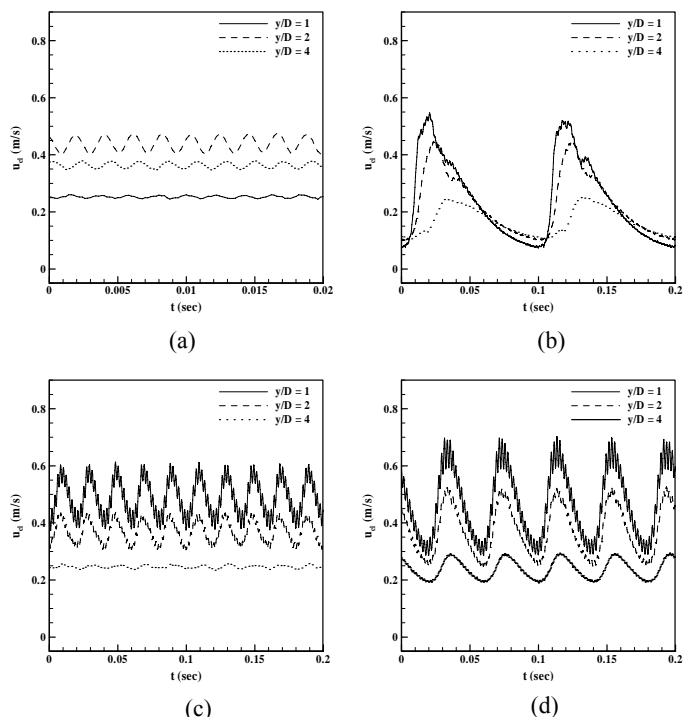


Fig. 3 Centreline ($x/D=0$) Velocity time trace at different axial locations (y/D) for (a) Unmodulated (b) AM at $f_{AM} = 10\text{Hz}$; (c) AM at $f_{AM} = 25\text{ Hz}$; (d) AM at $f_{AM} = 50\text{ Hz}$. The excitation voltage is set equal to 20 volts

D. Streamwise and wall normal velocity components

Fig. 5 – Fig. 9 show the effect of five actuation parameters on the streamwise component of mean velocity (u), its fluctuating component (u_{rms}), wall normal velocity (v), its fluctuating component (v_{rms}), and turbulent shear stress. Fig. 5 shows the nondimensional mean velocity (u -component) profiles along the interaction centerline at successive streamwise locations for 20 volts, 30 volts, 55 volts, 30 volts (with 10 Hz amplitude modulation) and 30 volts (with 50 Hz amplitude modulation) cases respectively. For each figure base flow profile at the corresponding location has been drawn for comparison. The effect of synthetic jet along the channel centerline extends up to higher wall-normal (y/D) distances for all cases. The strongest effect corresponds to the nearest streamwise location ($x/D = 5$). The near wall profiles for actuated flow are observed to be less effective at the intermediate streamwise locations. This suggests the periodic disturbance of the flow by actuation. Fig. 6 shows the u_{rms} variation in streamwise direction. The effect of actuation on rms profiles is observed to be more prominent in the near wall region as opposed to the mean velocity profiles (u).

Fig. 7 and Fig. 8 show the nondimensional mean velocity (v -component) and nondimensional rms velocity (v_{rms})

profiles along the channel centerline at different streamwise locations (x/D). For the base flow case, both mean and rms values of v -component are almost insignificant. Actuation effect can be clearly seen on the mean and rms profiles. It is important to note that in the streamwise direction, mean velocity profiles (v -component) show positive values, either less than base flow or higher than that. The v_{rms} profiles for all actuation parameters seem to have correlation with the u_{rms} profiles discussed earlier, and show almost similar variation. This indicates the fluctuations are increased in both the directions.

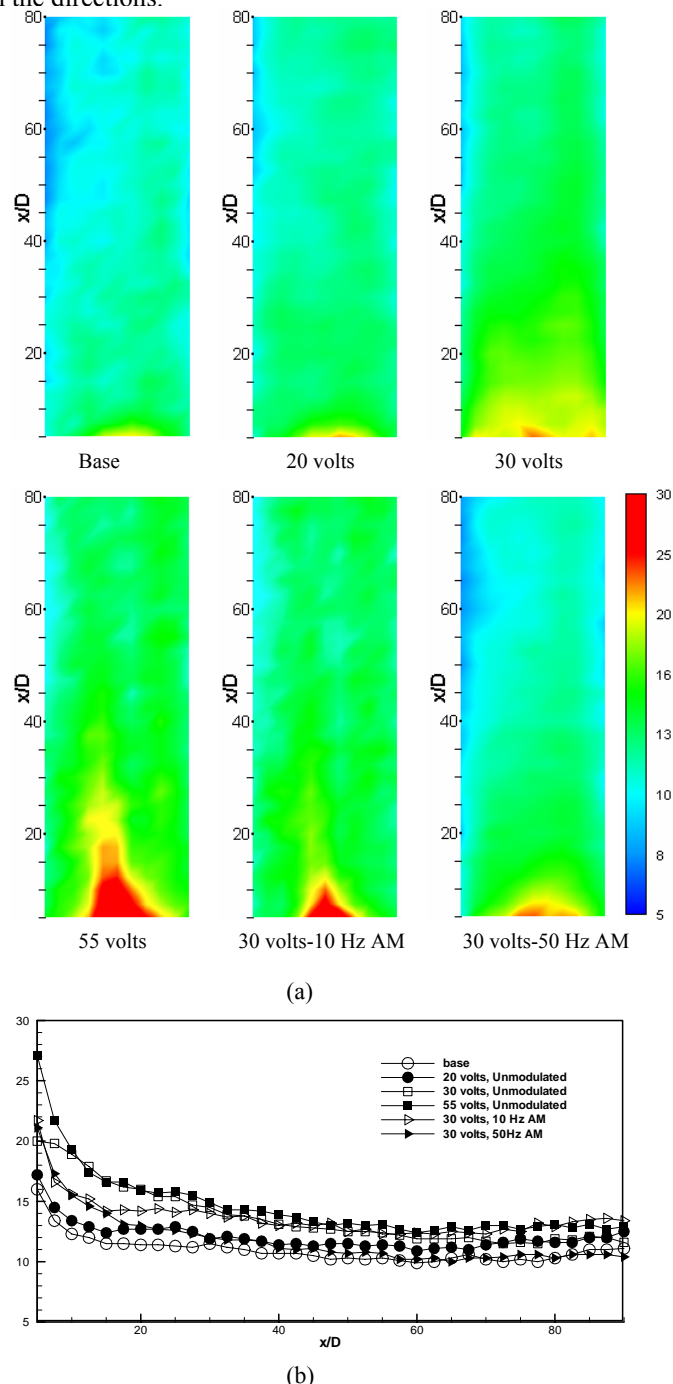


Fig. 4 (a) Heat transfer coefficient contour at different actuation voltages (b) Average heat transfer coefficient variation in streamwise direction at different actuation voltages

Fig. 9 shows the nondimensional turbulent shear stress profiles at various streamwise locations (x/D). This quantity represents cross correlation between the fluctuating

components of velocity (u' , v') and is equivalent to a shear stress. To a first approximation, one can expect similarity between $-\overline{u'v'}$ and $-\overline{T'v'}$, the latter being the turbulent heat flux. Thus augmentation in the former is a measure of enhancement in heat transfer itself. Still little variation in the near wall region can be attributed to the small spacing between the two streamwise vortices and measurements are averaged over the length of the hotwire.

E. Wall shear stress

The turbulent wall shear stress (τ_w) has been calculated at each location. The calculation of shear stress was carried out by fitting the law of the wall profile to the experimental data using least square method. The implicit equation found in terms of friction velocity (u_τ) was solved by Newton-Raphson root finding method, and using the friction velocity wall shear stress was calculated at each location.

Table 2 shows the percentage change in the value of wall shear stress at each location. A significant reduction in wall shear stress at most of the points has been observed. The maximum reduction at the locations under consideration is 15.46 %, which is expected to be more at some other location that has not been chosen for measurement. In Table 2 the values along the channel centerline have been shown. A reduction in shear stress is found for all actuation parameters in the streamwise direction only except 20 volts case. The effect of increasing jet strength with respect to the flow is justified by the increased reduction of shear stress for higher strength unmodulated jets. A striking feature of more reduction in shear stress at same actuation voltage of 30 volts for the two amplitude modulations is evident. This justifies the assumption of turbulence control by perturbing the flow around the bursting frequency.

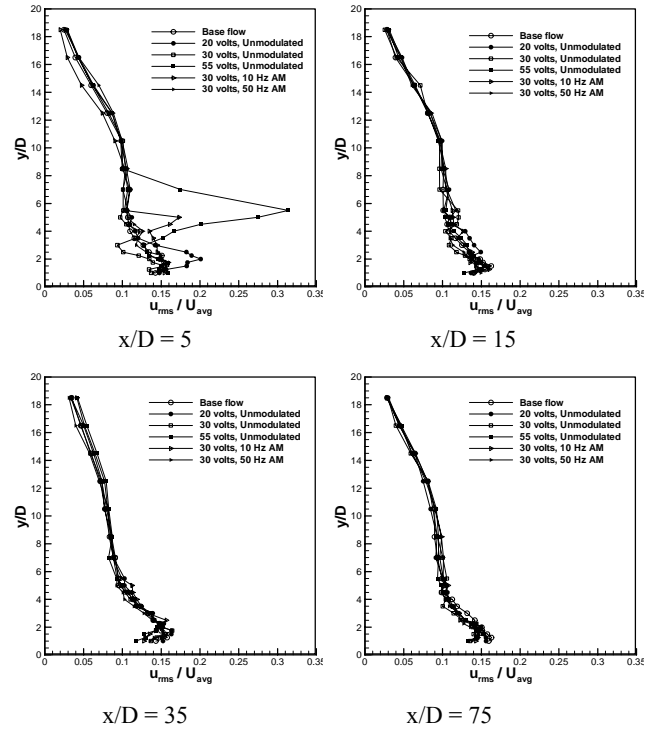


Fig. 6 Nondimensional rms velocity (u_{rms}) profiles at different streamwise locations (x/D) for various excitation conditions: 20 volts, unmodulated; 30 volts, unmodulated; 55 volts, unmodulated; 30 volts, 10 Hz AM; 30 volts, 50 Hz AM

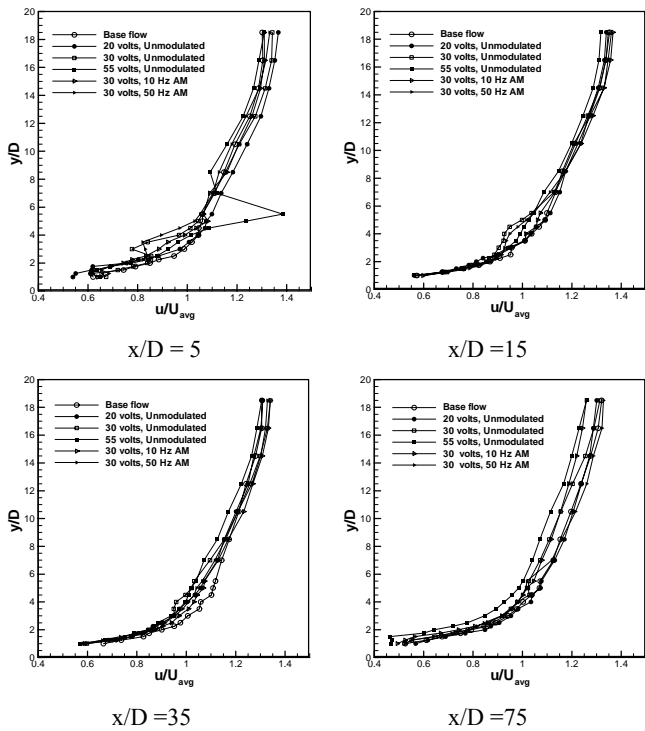


Fig. 5 Nondimensional mean velocity (u -component) profiles at different streamwise locations (x/D) for different actuation conditions: 20 volts, unmodulated; 30 volts, unmodulated; 55 volts, unmodulated; 30 volts, 10 Hz AM; 30 volts, 50 Hz AM

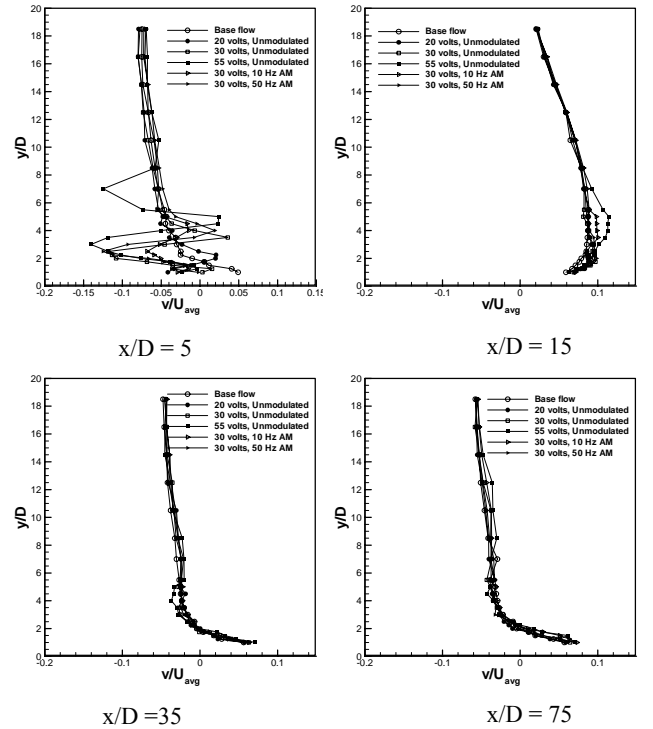


Fig. 7 Nondimensional mean velocity (v -component) profiles at different streamwise locations for various excitation conditions: 20 volts, unmodulated; 30 volts, unmodulated; 55 volts, unmodulated; 30 volts, 10 Hz AM; 30 volts, 50 Hz AM

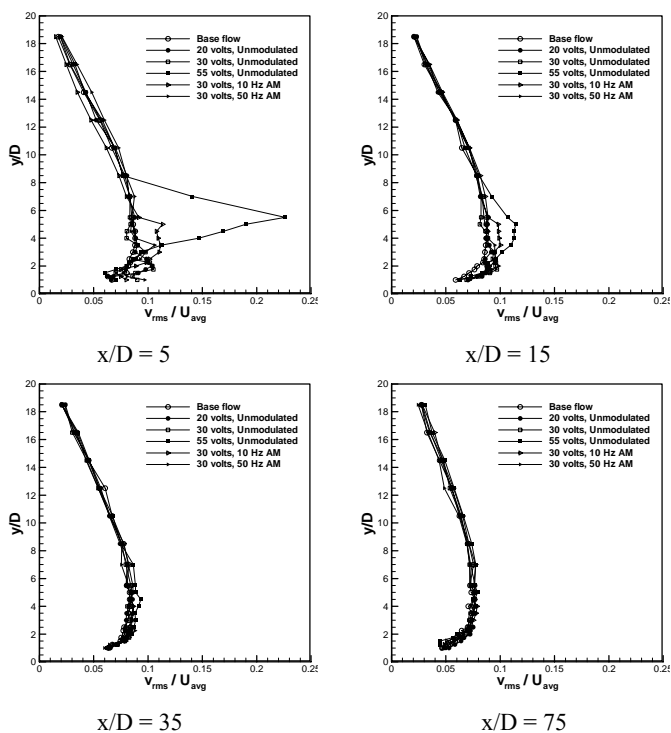


Fig. 8 Nondimensional rms velocity (v_{rms}) profiles at different streamwise locations for various excitation conditions: 20 volts, unmodulated; 30 volts, unmodulated; 55 volts, unmodulated; 30 volts, 10 Hz AM; 30 volts, 50 Hz AM

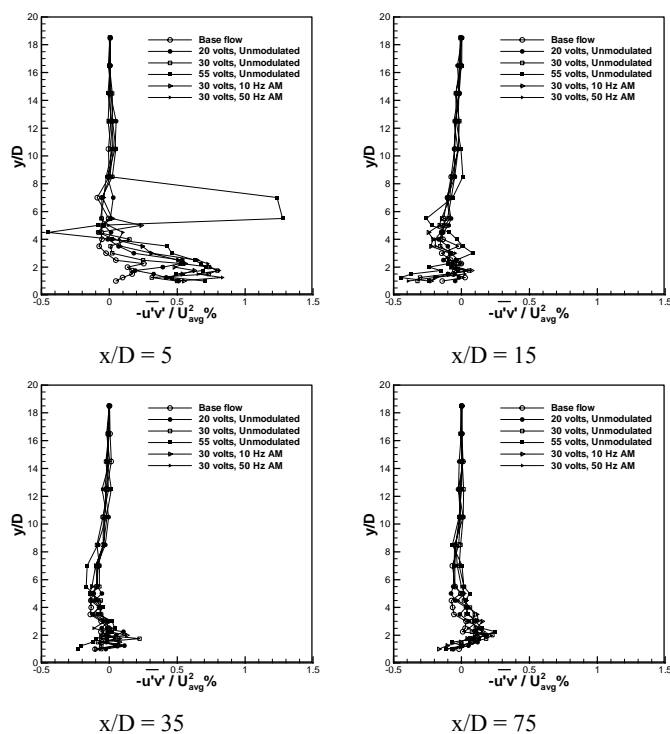


Fig. 9 Nondimensional turbulent shear stress profiles at different streamwise locations for various excitation conditions: 20 volts, unmodulated; 30 volts, unmodulated; 55 volts, unmodulated; 30 volts, 10 Hz AM; 30 volts, 50 Hz AM

TABLE 2

The percentage change in wall shear stress (τ_w) for actuated flow with respect to the base flow at various streamwise locations (x/D) at centerline ($z/D=0$)

X/D	20 VOLTS, NO AM	30 VOLTS, NO AM	55 VOLTS, NO AM	30 VOLTS, 10 HZ AM	30 VOLTS, 50 HZ AM
5	-1.40	-3.24	-0.55	-5.22	-7.50
15	-1.71	-5.04	-4.96	-0.25	-2.63
35	-5.64	-6.57	-9.04	-2.88	-5.24
55	1.08	-0.03	-6.88	-1.92	-8.82
75	1.52	-4.46	-15.46	-7.94	-2.75

IV. CONCLUSION

An experimental investigation to obtain quantitative information on synthetic jet actuation in a cross flow turbulent boundary layer has been undertaken. The synthetic jet is obtained by a piezoelectric actuator in cantilever arrangement with both sinusoidal and amplitude modulated excitation. Liquid crystal thermography and hotwire anemometry have been used. The following important observations are made.

(1) Amplitude modulation affects both spatial and temporal evolution of synthetic jets to a great extent. The magnitude of rms velocity fluctuations increase with amplitude modulated actuation.

(2) The cross flow mean and rms velocity profiles in streamwise direction show significant effect of synthetic jet actuation on turbulent boundary layers. The influence of synthetic jet actuation extends to further downstream distance for turbulent boundary layer.

(3) The synthetic jet reduces the wall shear stress which increases with increasing velocity ratio for unmodulated actuation whereas, for amplitude modulated case, the jet effectiveness significantly increases for the same energy input.

REFERENCES

- [1] R.M. Kelso, T.T.Lim, and A.E. Perry, "An Experimental study of Round Jets in Cross-Flow, J. Fluid Mech.", vol. 306, pp. 111-144, 1996.
- [2] B.A. Haven, and M. Kurosaka, "Kidney and anti-Kidney Vortices in Crossflow Jets", J. Fluid Mech., vol. 352, pp. 27-64, 1997.
- [3] L. Cortelezzi, and A.R. Karagozian, "On the Formation of the Counter-rotating Vortex Pair in Transverse Jets", vol. 446, pp. 347-373, 2001.
- [4] A. Glezer, "The Formation of Vortex Rings", Phys. Fluids, vol. 31, pp. 3532-3542, 1988.
- [5] M'Closkey, R.T. King, L. Cortelezzi, and A.R. Karagozian, "Actively Controlled Jet in Crossflow", J. Fluid Mech., vol. 452, pp. 325-335, 2002.
- [6] D. R. Smith, "Interaction of a synthetic jet with a cross flow boundary layer", AIAA Journal, vol. 40(11), pp. 2277-2288, 2002.
- [7] R. Rathnasingham, K. S. Breuer, "Active control of turbulent boundary layers", J. Fluid Mech., vol. 495, pp. 209-233, 2003.
- [8] I.M. Milanovic, K.B.M.Q. Zamman, "Synthetic Jets in Crossflow", AIAA Journal, vol. 43(5), pp. 929-940, 2005.